объединенный
институт
ядерных
исследований
дубна

E4-83-401

S.Cwiok,[1] I.N.Mikhailov, Ch.Briancon[2]

THE SHAPE OF FAST-ROTATING NUCLEI IN THE REGION OF SUBSHELL N = 82

Submitted to "Zeitschrift für Physik"

[1] Permanent address: Institute of Physics, Warsaw Technical University, Koszykowa 75, PL-00-662, Warsaw, Poland.

[2] Centre de Spectrométrie Nucléaire et de Spectrométrie de Masse, 91406 Orsay, France.

1983

1 - INTRODUCTION

The nuclear reactions with heavy ions allow to obtain the compound-nucleus states with angular momenta as high as $I \sim 60\text{-}80\ \hbar$ and with appreciable excitation energy. To analyse the experimental data, one needs the knowledge of the parameters characterizing the average self-consistent nuclear field, the deformation energy, the inertia properties of the nuclei, as well as the level-density of the excited nuclei.

The dependence of the nuclear shape on the rotational frequency has been studied theoretically by several authors. The effect of the rotation was investigated by Cohen, Plasil and Swiatecki [1] in the framework of the nuclear droplet model. The Dubna-Rössendorf collaboration [2], the Lund-Warsaw collaboration [3] and the Jülich group [4] carried out investigations of nuclear-shape properties at high angular momenta using the shell-correction method developed by Strutinsky [5]. In ref.[6] the combined effects of nuclear rotation and statistical excitation have been considered.

In the present work we investigate the fast-rotating nuclei in the vicinity of the magic neutron number N = 82. We focus our attention on "near-cold" nuclei (very small excitation energies) and discuss the influence of increasing the nuclear temperature on the shell-effects. We determine the spin-values at which oblate-to-prolate transition occurs in different erbium isotopes, as a function of the neutron number. We also illustrate the influence of shell-effects on the moment of inertia.

For the description of fast-rotating nuclei we employ the model developed in ref.[6]. The model unifies two different approaches : a method used in the description of fast-rotating cold nuclei[2-4] and a statistical approach for the determination of the properties of low-spin excitations. To simplify the model, we disregard the pairing correlations whose effects are important only at low temperatures ($t < 0.6$ MeV) and small angular momenta ($I < 25\text{-}30\hbar$).

2- DESCRIPTION OF THE MODEL AND CALCULATION RESULTS

Using the Strutinsky shell-correction method and averaging statistically the Routhian function $R(\beta,\omega,t)$ of a rotating nucleus, one obtains [1] :

$$R(\hat{\beta},\omega,t) = E_{LD}(\hat{\beta}) + \sum_{\nu} \varepsilon_{\nu}^{\omega}(\hat{\beta})\, \bar{n}_{\nu}(t) - \overline{\sum_{\nu} \varepsilon_{\nu}^{\omega=0}(\hat{\beta})\, \bar{n}_{\nu}(t=0)}. \qquad (1)$$

Here $\hat{\beta}$ is a set of deformation parameters, ω is the rotational frequency and t is the nuclear temperature. The liquid-drop component of the energy $E_{LD}(\hat{\beta})$ calculated in the droplet-model [7] is :

$$E_{LD}(\hat{\beta}) = E_S^{sph}\left[(B_S(\hat{\beta}) - 1) + 2x(B_C(\hat{\beta}) - 1)\right], \qquad (2)$$

where B_C and B_S describe the Coulomb and nuclear-surface energy, respectively, and are normalized so that they become unity for spherical nuclei :

$$E_S^{sph} = 17.9439\ \left[1-k\left(\frac{N-Z}{A}\right)^2\right]\ A^{2/3}\text{MeV} \qquad (3)$$

$$x = (Z^2/A)\ /\ \left[50.88\ \left(1-k\left(\frac{N-Z}{A}\right)^2\right)\right] \qquad (4)$$

$$k = 1.7826. \qquad (5)$$

The eigenvalues of the one-particle Routhian-function, $\varepsilon_{\nu}^{\omega}(\hat{\beta})$, are given by :

$$h^{\omega}(\hat{\beta})\ |\theta_{\nu}^{\omega}(\hat{\beta})\rangle = \varepsilon_{\nu}^{\omega}(\hat{\beta})\ |\theta_{\nu}^{\omega}(\hat{\beta})\rangle \qquad (6)$$

$$h^{\omega}(\hat{\beta}) = h(\hat{\beta}) - \omega j_x, \qquad (7)$$

where $h(\hat{\beta})$ is the one-particle hamiltonian of the self-consistent nuclear field. Eq.(1) can be written as :

$$\begin{aligned}
R(\hat{\beta},\omega,t) = E_{LD}(\hat{\beta}) &+ \\
&\Big[\sum_{\nu} \varepsilon_{\nu}^{\omega}(\hat{\beta})\, \bar{n}_{\nu}(t) - \sum_{\nu} \varepsilon_{\nu}^{\omega}(\hat{\beta})\, \bar{n}_{\nu}(t=0)\Big] + \\
&\Big[\sum_{\nu} \varepsilon_{\nu}^{\omega}(\hat{\beta})\, \bar{n}_{\nu}(t=0) - \overline{\sum_{\nu} \varepsilon_{\nu}^{\omega}(\hat{\beta})\, \bar{n}_{\nu}(t=0)}\Big] + \\
&\Big[\overline{\sum_{\nu} \varepsilon_{\nu}^{\omega}(\hat{\beta})\, \bar{n}_{\nu}(t=0)} - \overline{\sum_{\nu} \varepsilon_{\nu}^{\omega=0}(\hat{\beta})\, \bar{n}_{\nu}(t=0)}\Big] = \\
&R_{LD}(\hat{\beta},\omega) + U(\hat{\beta},\omega,t) + \delta R_{shell}(\hat{\beta},\omega,t=0).
\end{aligned} \qquad (8)$$

Here, $U(\hat{\beta},\omega,t)$ represents the excitation energy of the rotating nucleus

$$U(\hat{\beta},\omega,t) = \sum_{\nu} \varepsilon_{\nu}^{\omega}(\hat{\beta})\left[\bar{n}_{\nu}(t) - \bar{n}_{\nu}(t=0)\right] \qquad (9)$$

and $\delta R_{shell}(\hat{\beta},\omega,t=0)$ is the Strutinsky shell correction for a rotating nucleus at temperature $t = 0$:

$$\delta R_{shell}(\hat{\beta},\omega,t=0) = \sum_{\nu} \varepsilon_{\nu}^{\omega}(\hat{\beta})\, \bar{n}_{\nu}(t=0) - \overline{\sum_{\nu} \varepsilon_{\nu}^{\omega}(\hat{\beta})\, \bar{n}_{\nu}(t=0)}. \qquad (10)$$

The occupation numbers, $\bar{n}_{\nu}(t)$, are given by the Fermi distribution :

$$\bar{n}_{\nu}(t) = \{1 + \exp\left[(\varepsilon_{\nu}^{\omega}(\beta) - \bar{\lambda})/t\right]\}^{-1} \qquad (11)$$

with the chemical potential, $\bar{\lambda}$, determined by the number of particles (protons or neutrons) contained in the considered system :

$$\left.\begin{matrix}N\\Z\end{matrix}\right\} = \sum_{\nu} \bar{n}_{\nu}(t). \qquad (12)$$

The angular frequency ω and spin I are related by :

$$I = \sum_{\nu} (j_x)_{\nu\nu}\ \bar{n}_{\nu}(t), \qquad (13)$$

where the matrix elements, $(j_x)_{\nu\nu}$, are expressed in the representation of the eigenvectors of the Routhian-function (7).
$R_{LD}(\hat{\beta},\omega)$ is the Routhian of a rotating liquid drop :

$$R_{LD}(\hat{\beta},\omega) = E_{LD}(\hat{\beta}) - 1/2\ \omega^2\ \bar{J}(\hat{\beta},\omega). \qquad (14)$$

In the above formula the averaged moment of inertia $\bar{J}(\hat{\beta},\omega)$ is defined as :

$$-1/2\ \omega^2\ \bar{J}(\hat{\beta},\omega) = \overline{\sum_{\nu} \varepsilon_{\nu}^{\omega}(\hat{\beta})\ \bar{n}_{\nu}(t=0)} - \overline{\sum_{\nu} \varepsilon_{\nu}^{\omega=0}(\hat{\beta})\ \bar{n}_{\nu}(t=0)}. \qquad (15)$$

As is known, the moment of inertia averaged according to the Strutinsky shell-correction method using a velocity-independent nuclear field is close to the rigid-body value. It follows then that, for the Woods-Saxon self-consistent field, one obtains :

$$\bar{J}(\hat{\beta},\omega) \to J_{rig}(\hat{\beta}). \qquad (16)$$

In the statistical treatment of the properties of heated nuclei other thermodynamic potentials are also convenient :

a) The Gibbs-Routhian function :

$$F_R(\hat{\beta},\omega,t) = R(\hat{\beta},\omega,t) - tS(\hat{\beta},\omega,t), \qquad (17)$$

b) The Gibbs function (free energy) :

$$F(\hat{\beta},I,t) = F_R(\hat{\beta},\omega(I),t) + \omega(I)\, I \qquad (18)$$

and

c) the energy at a fixed value of the entropy :

$$E(\hat{\beta},I,S) = E(\hat{\beta},I,S=0) + U(\hat{\beta},\omega(I),t(S)), \qquad (19)$$

where $E(\hat{\beta},I,S=0)$ is the energy on the yrast line and $U(\hat{\beta},I,S)$ is the excitation energy above the yrast line at fixed spin I. The entropy of a heated nucleus is defined by :

$$S(\hat{\beta},\omega,t) = \sum_{\nu} \left[(\varepsilon_{\nu}^{\omega}(\hat{\beta}) - \bar{\lambda})\, \bar{n}_{\nu}(t)/t - \ell n(1-\bar{n}_{\nu}(t))\right]. \qquad (20)$$

The results presented in this paper have been obtained using the Woods-Saxon potential(8,9).

$$V(\vec{r},\hat{\beta}) = V_o/\left[1+\exp\ (\ \ell(\vec{r},\hat{\beta})/a)\right], \qquad (21)$$

where V_o is the depth of the potential-well and $\underline{a}$ is the diffuseness of the nuclear surface. The function $\ell(\vec{r},\hat{\beta})$, describing the distance between a given point $\vec{r}$ and the nuclear surface, has been determined numerically and taken negative for points inside the nucleus. For spherical nuclei : $\ell(r,\hat{\beta}=0) = r - R_o$, where $R_o = r_o\, A^{1/3}$ is the radius of the corresponding spherical nucleus.

The usual form of the spin-orbit interaction has been assumed :

$$V_{SO}(\vec{r},\hat{\beta}) = -\lambda \left(\frac{\hbar^2}{2MC}\right)\left[(\vec{\nabla}V\times\vec{p}).\vec{s}\right]_{r \to (r_o)_{SO}}, \qquad (22)$$

where $\vec{p}$ and $\vec{s}$ are nucleon momentum and spin operators respectively, and V is given by eq.(21) with $(r_o)_{SO}$ being the corresponding spin-orbit interaction radius given in the table.The Coulomb potential for protons has been determined as a classical electrostatic potential of a uniformly charged nucleus with a nuclear surface given by eq.(23) below, and a Coulomb radius of the central part of the potential : $(r_o)_C = 1.275$ fm .
The nuclear surface for moderate deformations can be expressed in the multipole expansion as :

$$R(\Omega,\hat{\beta}) = C(\hat{\beta})\, R_o\left[1+\sum_{L=2}^{4}\ \sum_{M=-L}^{L} \beta_{LM}\, Y^*_{LM}(\Omega)\right], \qquad (23)$$

where $\beta^*_{LM} = (-1)^M\, \beta_{L-M}$; Ω stands for the set of the polar angles (φ,θ).
The function $C(\hat{\beta})$ secures the conservation of the nuclear volume with the changes of nuclear surface.
One can choose a coordinate system in which :

$$\beta_{2\pm1} = 0, \quad \beta_{2+2} = \beta_{2-2} \qquad (24)$$

and introduce parameters β_2 and γ 10)

$$\beta_{20} = \beta_2 \cos\gamma$$
$$\beta_{22} = \beta_{2-2} = \frac{\beta_2}{\sqrt{2}} \sin\gamma\ . \qquad (25)$$

In such a parametrization of the quadrupole degrees of freedom, axially symmetric nuclear surfaces are described by $\gamma = k\frac{\pi}{3}$,(k = 0, ±1, ±2, ±3).
To extend this property to hexadecapole degrees of freedom we have used the Cayley-Hamilton theorem to write the spherical, rank-four tensor, β_{4M} as :

$$\beta_{40} = \frac{\beta_4}{6}\ (5\cos^2\gamma +1)$$
$$\beta_{42} = \beta_{4-2} = \frac{\beta_4}{6}\sqrt{\frac{15}{2}}\ \sin 2\gamma \qquad (26)$$
$$\beta_{44} = \beta_{4-4} = \frac{\beta_4}{6}\sqrt{\frac{35}{2}}\ \sin^2\gamma$$
$$\beta_{4\pm1} = \beta_{4\pm3} = 0\ .$$

A more general parametrization of the hexadecapole deformation has been suggested recently in ref.(11).
This leaves us with a set of three independent deformation parameters, $\hat{\beta} = (\beta_2,\beta_4,\gamma)$. Since the full minimization with respect to the hexadecapole deformation parameter β_4 is practically beyond our technical possibilities, its value has been inferred from the minimization of the liquid drop energy with respect to β_4 for a prolate ($\gamma = 0°$, rotation around the axis perpendicular to the symmetry axis) and an oblate shape ($\gamma = -60°$, rotation around the symmetry axis).

Fig.1 presents the dependence of β_4 on β_2 for $\gamma = 0°$ and $\gamma = -60°$, for two spin-values : I = 0 and I = 60. It can be seen that the difference between the equilibrium deformations for I = 0 and I = 60 is not very significant. Thus, in the subsequent calculations the hexadecapole deformation β_4 has been deduced from its equilibrium value for the liquid-drop at I = 0. The values of β_4 for $0° > \gamma > -60°$ have been determined by a linear interpolation at fixed β_2.

All calculations presented in this paper have been carried out using the level spectrum of ^{158}Er. The relevant values of parameters are listed in Table I.

The calculations were carried out for even isotopes of erbium : $^{146-154}Er$ and ^{158}Er. The heaviest of the studied isotopes represent a stably deformed nucleus, the lighter ones represent the transitional nuclei. The position of these nuclei in the periodic table makes them an interesting field of investigation , both for the theorists and experimentators.

The results of our calculations for the energy surfaces are given in figs. 2-9. Each of the figures shows several energy surfaces obtained for different characteristic values of the spin. The results are presented in triangular plots as contour lines in the β_2-γ plane. The parameter β_2 measures the distance from a given point in the plot to the left vertex. The angle γ changes from $\gamma = 0°$ at the lower edge (a prolate nucleus rotating around the axis perpendicular to the symmetry axis of the field) to $\gamma = -60°$ at the upper edge (the oblates shape with coinciding symmetry and rotation axes). The lines in the plots are contour-lines corresponding to a given equal free-energy. The interval separating the neighbouring lines is 0.5 MeV. The "valleys" in the free-energy landscape are indicated by shaded areas, the darker ones corresponding to the deeper depression.

Most of the calculations were performed for t = 0.2 MeV. Such value of the temperature does not destroy the shell-effects and, at the same time,facilitates the interpolation procedure used in the calculations. The effects of statistical excitation were studied for ^{154}Er at temperatures t = 0.6 MeV and t = 1.2 MeV. Comparing our figures one can see that the shell effects enrich the structure of the energy surfaces, leaving the positions of the main minima at about the same place. At t = 0.2 MeV the shell effects generate very complicated free-energy surfaces, at t = 0.6 MeV the low-scale variations of the energy are already washed out, and at t = 1.2 MeV the shell effects are not seen in the energy surfaces at all. A more detailed information concerning the spin-dependence of the equilibrium deformation is given in figs. 10 and 11. The above-mentioned tendencies can be seen from these figures too. Figs. 12 and 13 show the moment of inertia of $^{148,154}Er$ as a function of ω^2. The large-scale variations of the moments of inertia are related to the changes in the nuclear shape. Such changes appear as combined effects of the shell and the liquid-drop forces. The additional shell-effects, not related to the shape transitions, are also visible in the figures as low-scale fluctuations disappearing at moderate temperatures (t = 0.6 MeV). At high temperatures there remains a large

bump in the moment of inertia, corresponding to the transition from the oblate to the three-axial close-to-prolate configurations.

The shell effects determine also the critical value of spin at which the oblate-to-prolate transition takes place. As is seen in fig. 14, the dependence of such spin values on the neutron number N is rather strong : it increases from around 40ħ to more than 70ħ when going from ^{146}Er to ^{154}Er. Similar conclusions are obtained in ref.12), although our values for such spins are somewhat larger as compared to those of ref.12).

Calculations of the nuclear shape properties in ^{154}Er are also reported in ref.13) for zero temperature. The comparison of fig.6 in the present work (T = 0.2 MeV) with fig.11 in ref.13) shows a qualitative agreement of these calculations.

As is seen in figs.2-9, the free energy surfaces have more than one minimum for small temperatures. Such is the situation in ^{154}Er. The energies of states in ^{154}Er corresponding to different minima are shown in fig.15 as functions of the spin. One sees that the yrast-line in this nucleus consists of several lines : the deformation changes slowly with the spin in each of these lines, but undergoes a rather drastic change with the change of the yrast configuration.

It is useful to present the results by calculating the rotational frequency $\omega_{rot}(I)$ as a function of the nuclear spin for each of the configurations lying in the vicinity of the yrast line. The rotational frequency determines the energy spacings of the states with different values of spins belonging to such configurations. If one considers the stretched quadrupole γ-transitions with $\Delta I = 2$ which go along the yrast line or along the lines corresponding to other low-lying configurations, one has for the energy of γ-quanta the expression $E_\gamma(I) = 2\,\omega_{rot}(I)$.

As an example in fig.16 we present the energies of stretched E2 γ-quanta as functions of the spin for ^{154}Er. The different curves in fig.16 correspond to the energies of γ-rays cascading along the different configurations shown in fig.15. The number of γ-rays in a given interval of energy which are emitted from the high-spin states is related to the slope of the curves. A plateau may be associated with an accumulation of γ-rays with the same energy. The same is expected for those values of $E_\gamma(I)$ which correspond to more than one curve, because in this case, one may envisage the emission of γ-rays in cascades going along different lines.

Thus the irregularities in the curves in fig.16 (in particular, the position of plateaux) may be associated with the bumps in the intensity spectra of γ-rays emitted from the high-spin nuclear states. The spectra of quasi-continuous γ-rays following (HI,xn) reactions are known experimentally in a number of cases. Strong irregularities in the intensity of γ-rays, $n_\gamma(E_\gamma)$, are found in the case of the nucleus ^{154}Er [14-20] : the cascade starting in the region of spins of about I ~ 60-70 ħ produces the spectrum of γ-rays with $n_\gamma(E_\gamma)$ having two strong bumps. The positions of the two maxima of $n_\gamma(E_\gamma)$ are indicated in fig.16 by dotted lines. As is seen, these positions may be explained, at least partially, by the spin dependence of the energies of different nuclear configurations.

3 - CONCLUDING REMARKS

In this paper we investigated theoretically the erbium isotopes from the well-deformed to the quasi-spherical regions. The evolution of the shape of the nuclear surface has been studied as a function of spin for different number of neutrons ($78 \leqslant N \leqslant 90$).

The erbium isotopes studied in this paper are interesting from the point of view of experiments in which the multiplicity and energy distributions of γ-quanta following the (HI,xn) reaction are measured. Such experiments have been done during the last years [14-20]. As is shown above the shape variations and the resulting changes in the nuclear moment of inertia determine the spectrum of that part of the γ-spectrum which corresponds to the yrast cascade in the nucleus obtained in the fusion process. A more detailed analysis of the γ-spectra obtained in the C.S.N.S.M. (Orsay) [16,17] and based on the calculations reported here is in progress.

The authors express their gratitude to Dr. H. Lizurej and Dr. J.P. Thibaud for the interest in the work and for the help in preparing the manuscript.

This work has been done in the framework of the IN2P3-JINR collaboration agreement ; one of the authors (S.C.) takes this opportunity to thank the staff and administration of C.S.N.S.M. (Orsay) for creating pleasant conditions at Orsay during the work on the topic of the paper.

TABLE

Parameters of the average field potential for ^{158}Er

	Central potential			Spin orbit interaction		
	r_o (fm)	a (fm)	V_o (MeV)	$(r_o)_{so}$ (fm)	a_{so} (fm)	λ
protons	1.275	0.70	-55.5	0.901	0.70	18.9
neutrons	1.347	0.70	-43.7	1.221	0.70	33.3

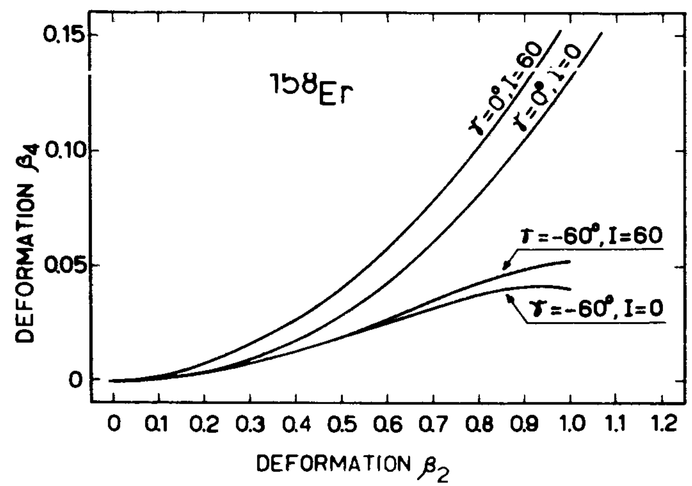

Fig. 1 : The dependence β_4 on β_2 for the prolate (γ=0°) and oblate (γ=60°) shapes resulting from the minimization of the liquid-drop energy. Calculations correspond to ^{154}Er and are shown for two values of the spin (I=0 and I=60ħ) indicated at the lines.

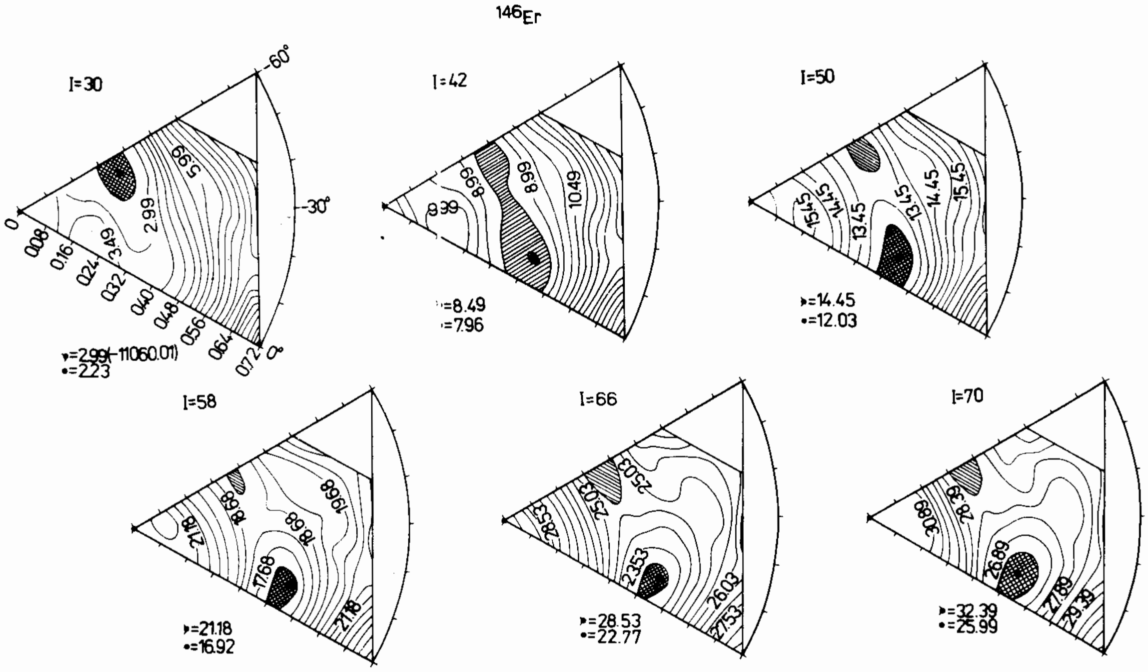

Fig.2: The free-energy surfaces for ^{146}Er in a β_2-γ plane. The left vertex corresponds to the spherical shape (β =0). The prolate configurations rotating perpendicular to the symmetry axis are represented by the lower edge of the triangular charts ($\gamma = 0°$).The oblate configurations rotating around the symmetry axis are represented by the upper edge (γ=-60°). The distance between the lines correspods to 0.5 MeV. The valleys in the landscape are indicated by shaded areas, the darker ones corresponding to deeper minima. Below the plots the values of the free-energy of spherical configuration (>) and at the minimum (•) are given. Here and in the following figures the temperature is taken t = 0.2 MeV if not stated otherwise.

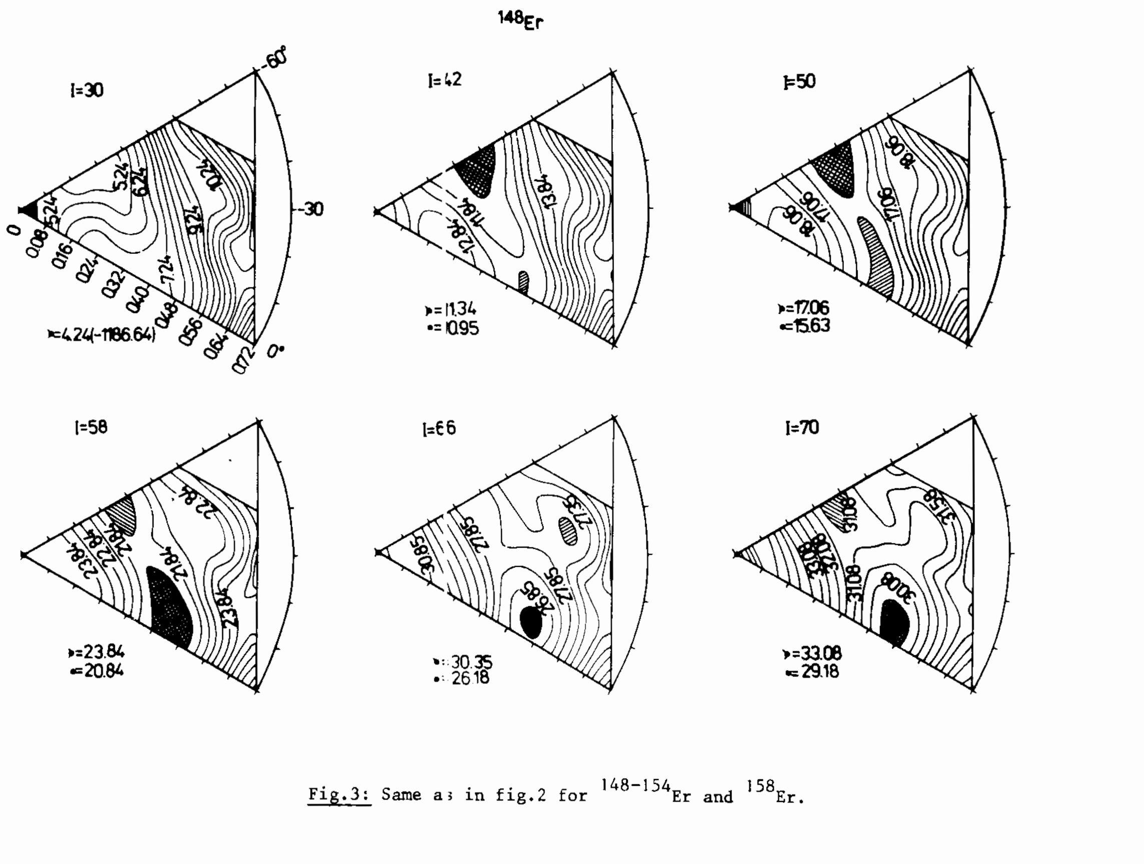

Fig.3: Same as in fig.2 for $^{148-154}$Er and ^{158}Er.

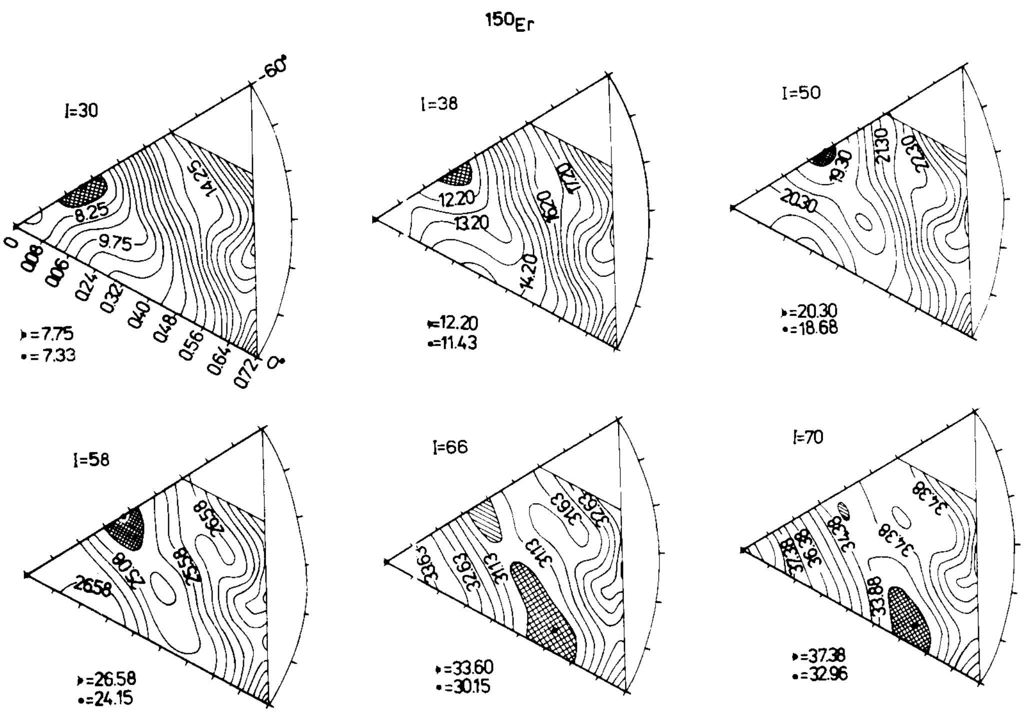

Fig.4: Same as in fig.2 for $^{148-154}Er$ and ^{158}Er.

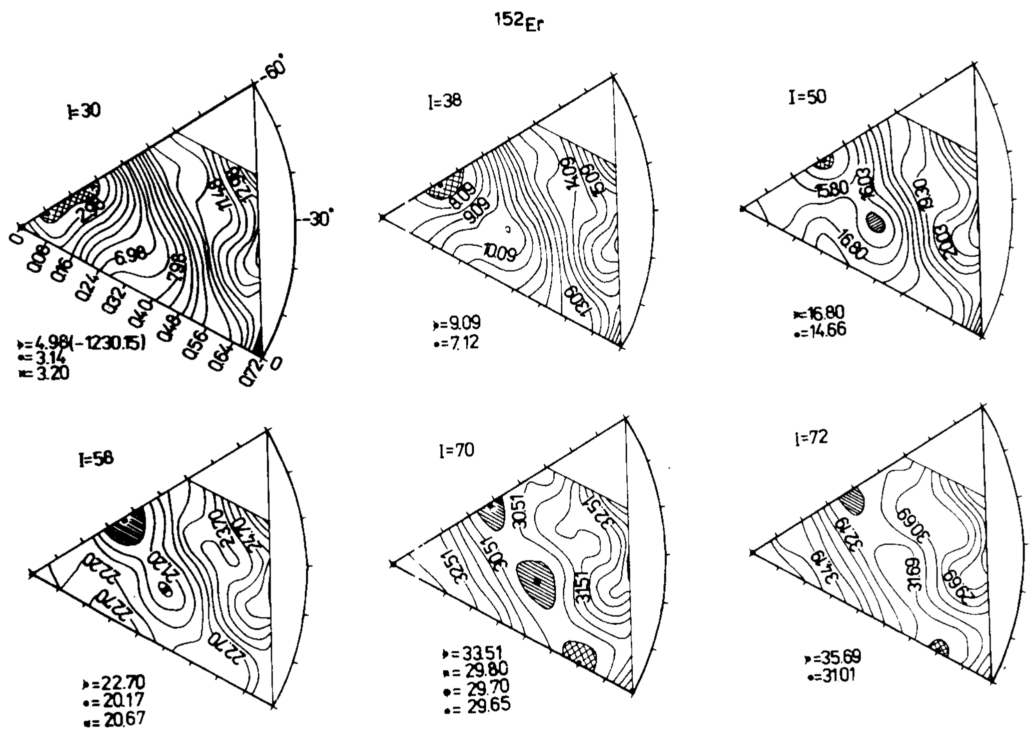

Fig.5: Same as in fig.2 for $^{148-154}Er$ and ^{158}Er.

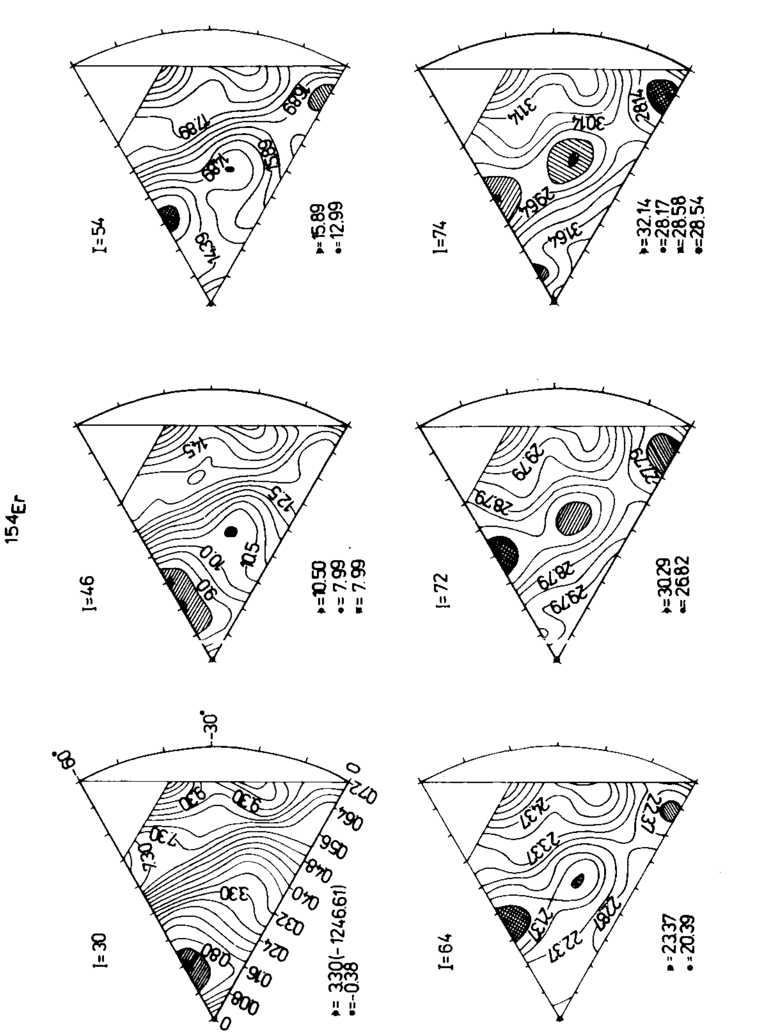

Fig.6: Same as in fig.2 for $^{148-154}Er$ and ^{158}Er.

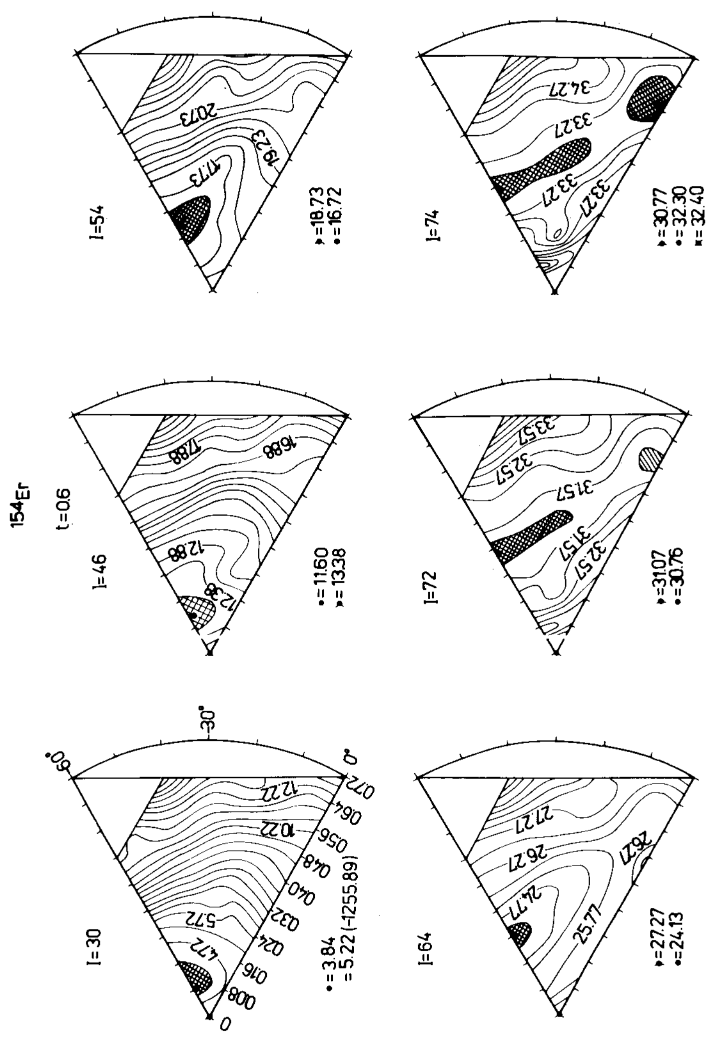

Fig.7: Same as in fig.2 for $^{148-154}Er$ and ^{158}Er.

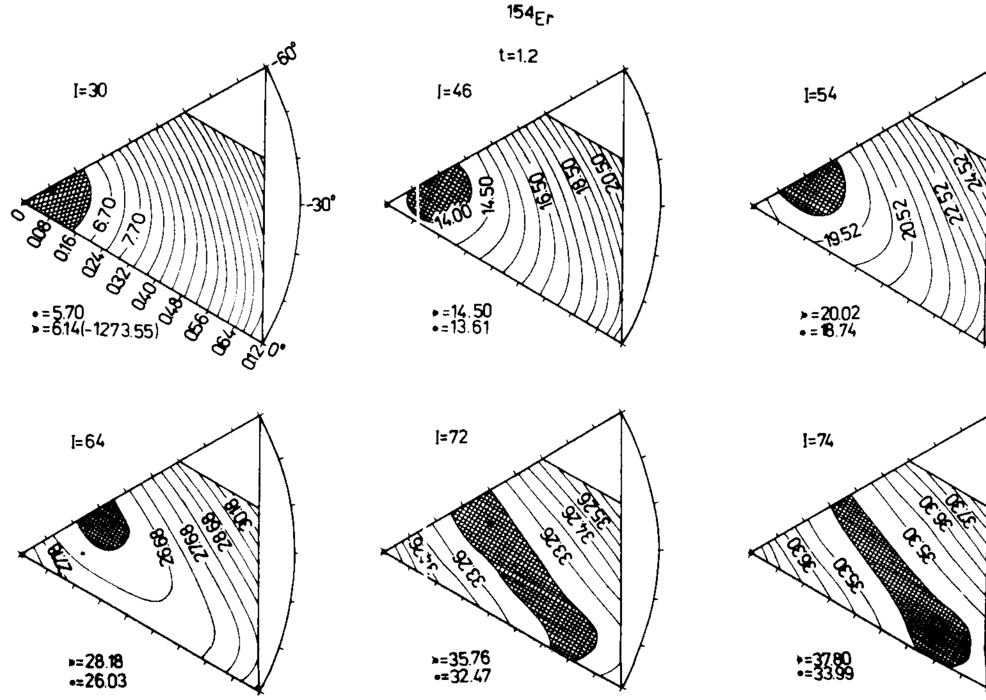

Fig.8: Same as in fig.2 for $^{148-154}Er$ and ^{158}Er.

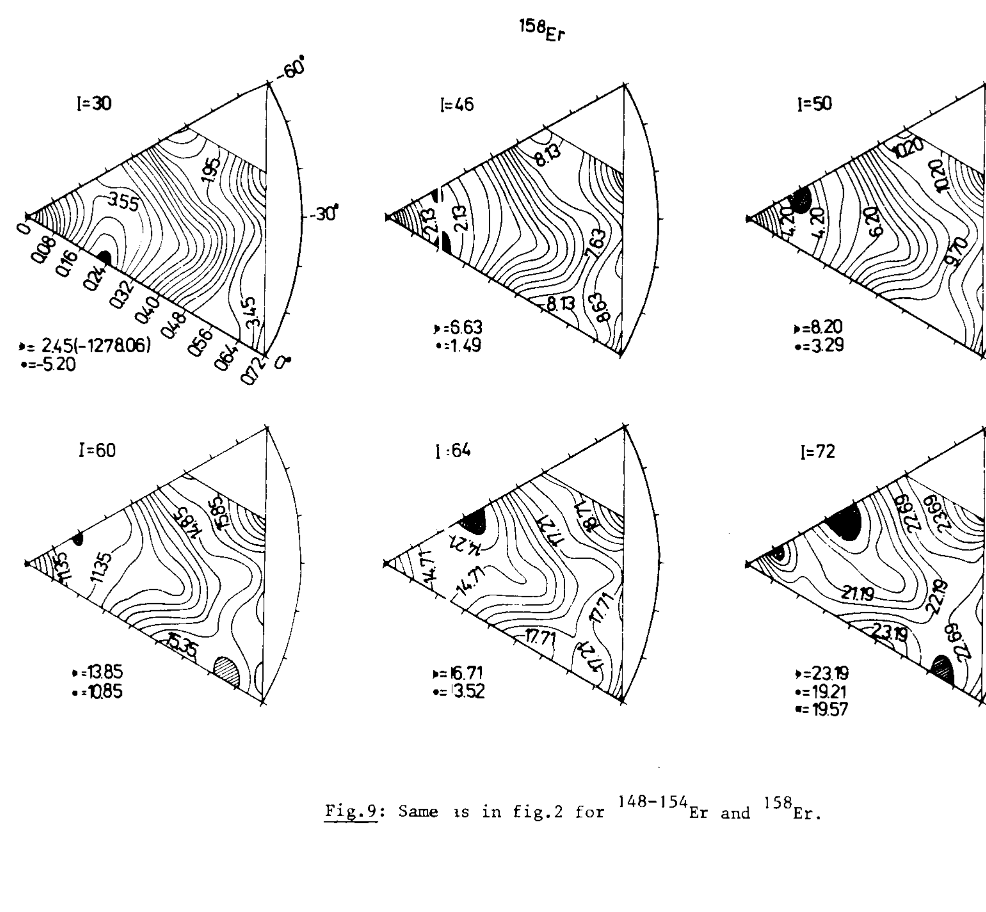

Fig.9: Same is in fig.2 for $^{148-154}Er$ and ^{158}Er.

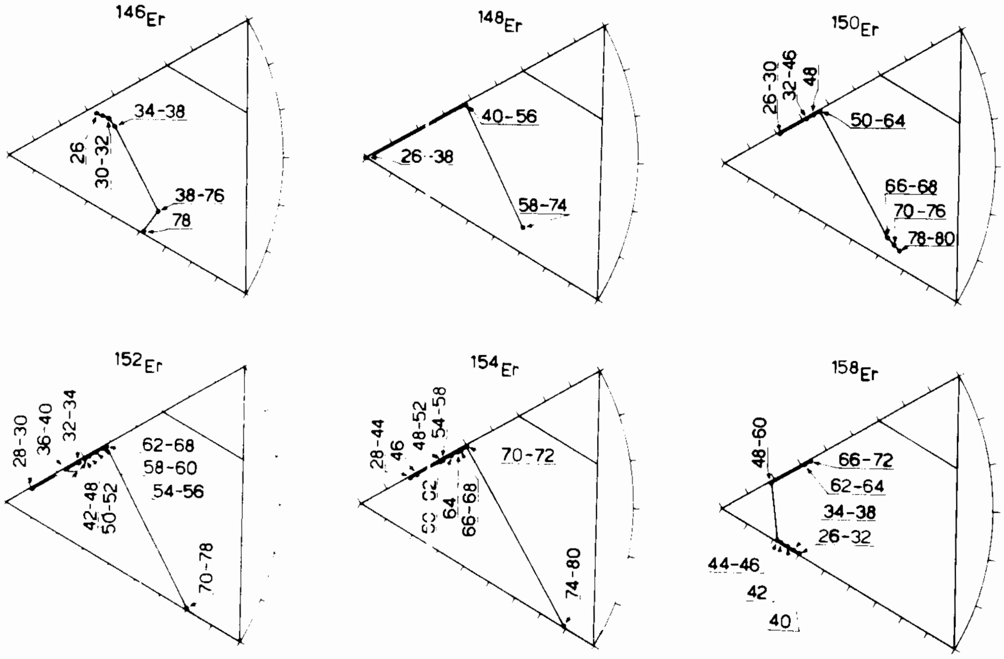

Fig. 10 : The hodograph for the deepest free-energy minimum for $^{146-154}$Er and ^{158}Er at t = 0.2 MeV. The points and the numbers by them indicate the position of the minimum and the corresponding value of spin.

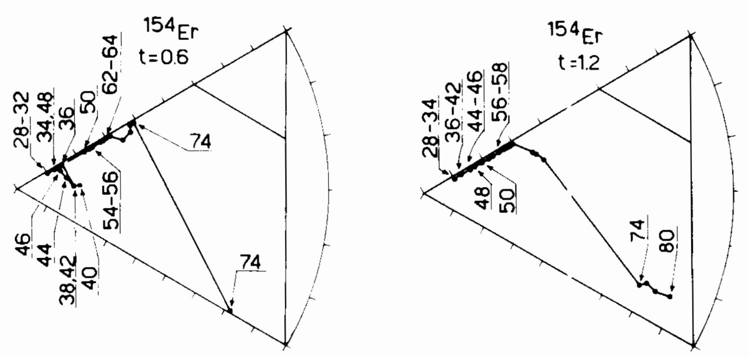

Fig. 11 : Same as in fig. 10 for ^{154}Er at t = 0.6 MeV and t = 1.2 MeV.

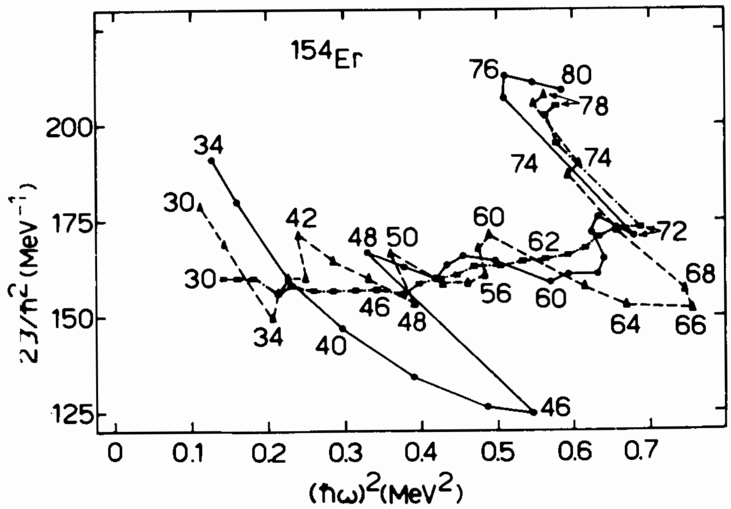

Fig.12: The moment of inertia as a function of the square of the rotational frequency for ^{154}Er at different temperatures:
t = 0.2 MeV - solid line with dots.
t = 0.6 MeV - dashed line with triangles,
t = 1.2 MeV - dotted line with squares.
The numbers at the marks on the lines indicate the spin values.

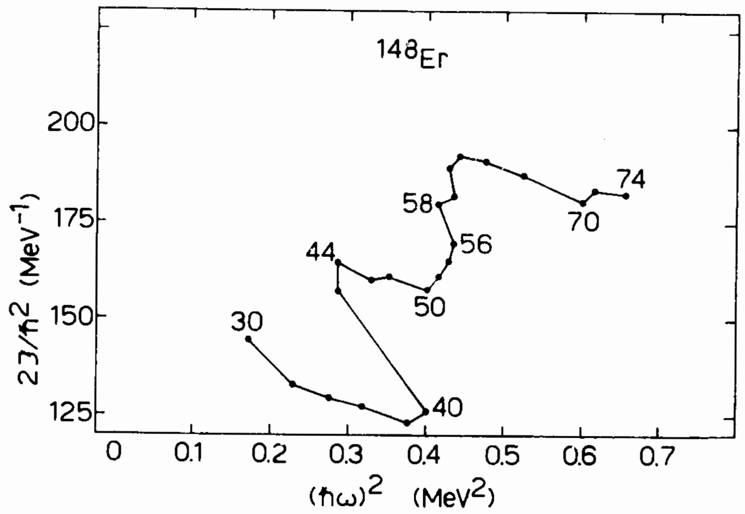

Fig. 13 : The moment of inertia as a function of the square of the rotational frequency for ^{148}Er. (temperature t = 0.2 MeV).

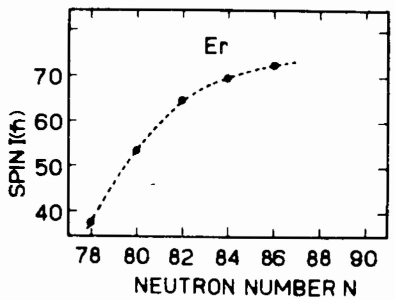

Fig. 14 : The value of the spin I, at which the oblate-to-prolate transition occurs, given as a function of the neutron number for Erbium isotopes.

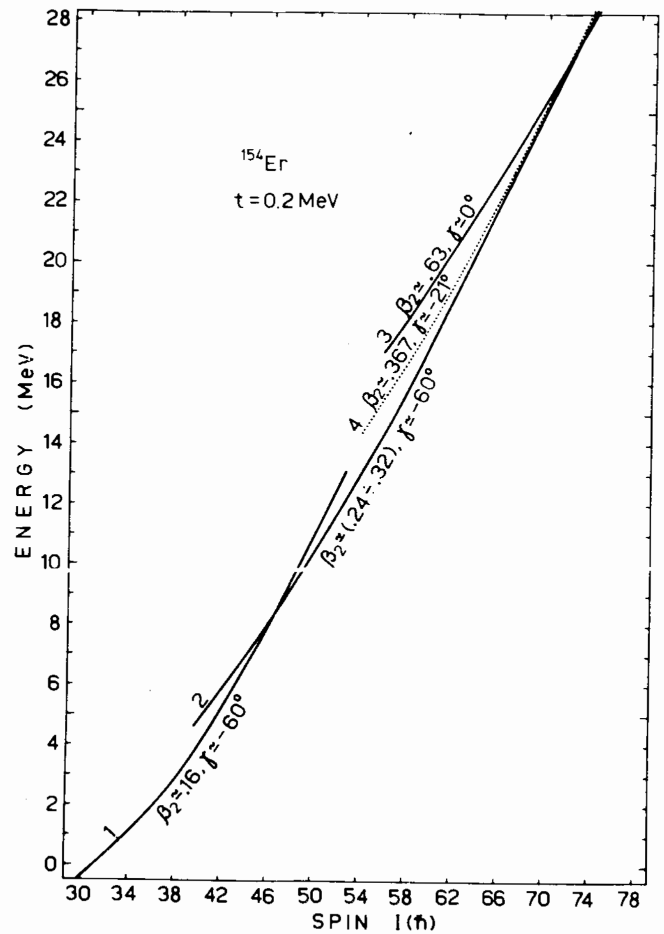

Fig. 15 : The structure of the yrast-line in ^{154}Er (T = 0.2 MeV)

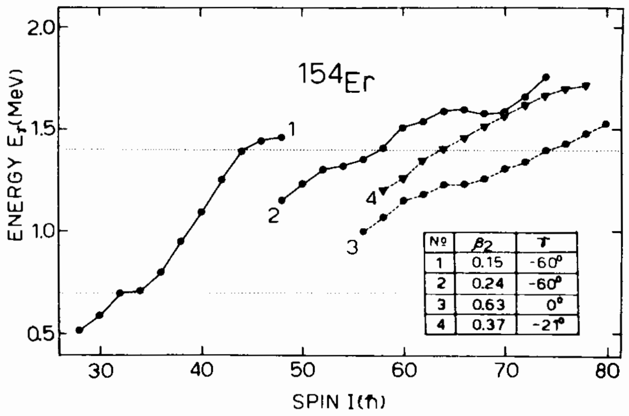

Fig. 16 : Energies of the stretched E2 transitions along the different configurations in ^{154}Er shown in fig.15.

REFERENCES

(1) S. Cohen, F. Plasil and W.J. Swiatecki, Ann. of Phys. 82 (1974) 557

(2) K. Neergård and V.V. Pashkevich, Phys. Lett. 59B (1975) 218
K. Neergård, V.V. Pashkevich and S. Frauendorf, Nucl. Phys. A262 (1976) 61.

(3) R. Bengtsson, S.E. Larsson, G. Leander, P. Möller, S.G. Nilsson, S. Aberg and Z. Szymanski, Phys. Lett. 57B (1975) 301
G. Andersson, R. Bengtsson, S.E. Larsson, G. Leander, P. Möller, S.G. Nilsson, I. Ragnarsson, S. Aberg, J. Dudek, B. Nerlo-Pomorska, K. Pomorski and Z. Szymanski, Nucl. Phys. A268 (1976) 205

(4) K. Neergård, H. Toki, M. Ploszajczak and A. Faessler, Nucl. Phys. A287 (1977) 48.

(5) M. Brack, J. Damgaard, A.S. Jensen, H.C. Pauli, V.M. Strutinsky and C.Y. Wong, Rev. Mod. Phys. 44 (1972) 320

(6) A.V. Ignatyuk, I.N. Mikhailov, L.H. Molina, R.G. Nazmitdinov and K. Pomorski, Nucl. Phys. A346 (1980) 191.

(7) W.D. Myers and W.J. Swiatecki, Arkiv. Fysik 36 (1967) 343.
W.D. Myers and W.J. Swiatecki, Ann. Phys. (N.Y.) 55 (1969) 395.
W.D. Myers, Droplet Model of Atomic Nuclei (IFI/Plenum, New-York 1977)

(8) J. Dudek and T. Werner, J. Phys. G4 (1978) 1543.

(9) J. Dudek, A. Majhofer, J. Skalski, T. Werner, S. Cwiok and W. Nazarewicz, J. Phys. G5 (1979) 1359.

(10) A. Bohr, Mat. Fys. Medd. Dan. Vid. Selsk., 26 (1952) N°14

(11) S.G. Rohozinski and A. Sobiezewski, Acta Phys. Pol. B12 (1981) N°10

(12) I. Ragnarsson, T. Bengtsson, G. Leander and S. Aberg, Proc. of the Int. Conf. on "Band Structure and Nuclear Dynamics", Tulane-University, New-Orleans, Nucl. Phys. A347 (1980) 287

(13) S. Aberg, S.E. Larsson, P. Möller, S.G. Nilsson, G. Leander and I. Ragnarsson, Symp. on Physics and Chemistry of Fission, Jülich 1979, Vol.1, p.303

(14) H.J. Körner, D.L. Hillis, C. Roulet, P. Aguer, C. Ellegaard, D.B. Fossan, D. Habs, M. Neiman, F.S. Stephens and R.M. Diamond, Phys. Rev. Lett. 43 (1979) 490

(15) M.A. Deleplanque, J.P. Husson, N. Perrin, F.S. Stephens, C. Bastin, C. Schück, J.P. Thibaud, L. Hildingsson, S. Hjorth, A. Johnson and Th. Lindblad, Phys. Rev. Lett. 43 (1979) 1001.

(16) P. Aguer, G. Bastin, A. Péghaire, J.P. Thibaud, N. Perrin, H. Sergolle and Ph. Hubert, Berkeley Conference (1980).

(17) P. Aguer, G. Bastin, A. Péghaire, J.P. Thibaud, N. Perrin, H. Sergolle and Ph. Hubert, Nobel Symposium on nuclei at very high spin, Physica Scripta, 24 (1981) 140.

(18) R.M. Diamond and F.S. Stephens. Nuclei at high angular momentum. Ann. Rev. Nucl. Part. Sci. 30 (1980) 85.

(19) P. Chowdhury, J. Borggreen, T.L. Khoo, I. Ahmad, R.K. Smither, S.R. Faber, P.J. Daly, C.L. Dors and J. Wilson, Phys. Rev. Lett. 47 (1981) 778.

(20) F. Folkmann, J.D. Garrett, G.B. Hagemann, M.N. Harakeh, B. Herskind, D.L. Hillis, S. Ogaza, H. Emling, E. Grosse, D. Schwalm, R.S. Simon and P.O. Tjøm, Nucl. Phys. A361 (1981) 242.

Received by Publishing Department
on June 13,1983.

WILL YOU FILL BLANK SPACES IN YOUR LIBRARY?

You can receive by post the books listed below. Prices - in US $, including the packing and registered postage

Цвек С., Михайлов И.Н., Бриансон Ш.

E4-83-401

Форма быстровращающихся атомных ядер из окрестности магической оболочки N = 82

Используя метод оболочечной поправки Струтинского, исследованы быстровращающиеся ядра изотопов эрбия из окрестности магической оболочки N = 82. В качестве среднего поля использован потенциал Вудса-Саксона с учетом неаксиальной гексадекапольной деформации. Рассчитаны параметры равновесных деформаций и моменты инерции при разных значениях спинов ядер. Исследовано влияние нагревания ядра на его оболочечные эффекты.

Работа выполнена в Лаборатории теоретической физики ОИЯИ.

Препринт Объединенного института ядерных исследований. Дубна 1983

Cwiok S., Mikhailov I.N., Briancon Ch.

E4-83-401

The Shape of Fast-Rotating Nuclei in the Region of Subshell N = 82

The fast rotating erbium nuclei in the vicinity of N = 82 are investigated in the framework of the Strutinsky shell-correction method using the Woods-Saxon potential including non-axial hexadecapole deformations. The equilibrium deformation and moment of inertia are calculated for different spin values. The influence of nuclear temperature on the shell-effects is also discussed.

The investigation has been performed at the Laboratory of Theoretical Physics, JINR.

Preprint of the Joint Institute for Nuclear Research. Dubna 1983